



Contents lists available at ScienceDirect

## Journal of Industrial and Engineering Chemistry

journal homepage: [www.elsevier.com/locate/jiec](http://www.elsevier.com/locate/jiec)

# Do film reactions affect ozone gas–liquid fast-moderate reaction kinetics in the proximity of gas–water interface?

F.J. Beltrán, F.J. Rivas\*

Departamento de Ingeniería Química y Química Física, Instituto Universitario de Investigación del Agua, Cambio Climático y Sostenibilidad, Universidad de Extremadura, 06006 Badajoz, Spain

## ARTICLE INFO

## Article history:

Received 12 April 2023

Revised 9 June 2023

Accepted 2 July 2023

Available online 13 July 2023

## Keywords:

Water Ozonation

Kinetic modeling

Film theory

Penetration theory

Direct ozone reaction

Hydroxyl radical reaction

## ABSTRACT

Kinetics of the ozonation of water contaminants is usually based on mol balance equations applied in the water bulk. In these models, direct and free radical reactions are considered, neglecting the contribution of reactions developed in the proximity of the gas–water interface. In this work, a theoretical kinetic model of the ozonation involving direct and free radical reactions in the film and water bulk is carried out. The model is based on film and penetration absorption theories. Time concentration profiles are assessed by coupling the non-stationary penetration theory with bulk mass balances. Studied variables are chosen according to their influence on the numbers of Hatta and instantaneous reaction factor. These parameters are equilibrium ozone and compound concentrations, direct rate constant, and mass transfer coefficient. The effect of pH and hydrogen peroxide are studied. Calculated results reveal that direct reaction contribution in the film has a significant importance, especially in fast-moderate kinetic regimes of ozone absorption. Absence of film free radical reactions leads to compound removal rates slightly lower than the complete mechanism (fast regimes develop). Formation of hydrogen peroxide and its reaction with ozone leads to the formation of free radicals.

© 2023 The Author(s). Published by Elsevier B.V. on behalf of The Korean Society of Industrial and Engineering Chemistry. This is an open access article under the CC BY-NC-ND license (<http://creativecommons.org/licenses/by-nc-nd/4.0/>).

## Introduction

Nowadays, ozone can be accepted as a classical oxidant in water treatment. Ozone is mainly applied to reduce the formation of organo-halogen compounds during chlorine disinfection in drinking water treatment plants [1,2] but also it can be used to remove contaminants of emerging concern, such as many pharmaceuticals from urban wastewater effluents [3–5]. In these ozone-based processes, contaminants can be eliminated through direct reactions with molecular ozone and/or reactions with hydroxyl radicals formed from ozone decomposition [6,7]. While direct ozone reactions are very selective and depend on the presence of specific groups in the organic molecules (i.e. OH groups in phenols), free radical reactions are non-selective. Hence corresponding free radical rate constants are extremely high, regardless of the nature of organics, especially for the case of molecules of many pharmaceuticals or precursors of organo-halogen compounds [8–10]. The importance of this secondary pathway of ozone action depends on the presence of other substances such as carbonates and/or other oxidants (mainly hydrogen peroxide), light (mainly UV radi-

ation) and catalysts [11,12]. As a rule of thumb, carbonates will inhibit the oxidation of organics by scavenging the generated free radicals. Contrarily, the second agents accelerate the formation of free radicals promoting or catalyzing ozone decomposition towards these short live species of high oxidizing power. These latter processes take part of the group named as advanced oxidation processes (AOP) [13,14].

Accordingly, due to the increasing importance of ozone processes, kinetic modeling has attracted the interest of researches reporting works where the kinetic of ozone reactions plays a fundamental role [15,16]. However, kinetic equations, included in mass balances, consider mass transfer effects based on a mass transfer coefficient without contemplating any enhancement of ozone absorption in the proximity of the gas–water interface. Usually, ozone mass transfer rate from the gas to the water bulk is exclusively attributed to the product of the mass transfer coefficient and the ozone concentration driving force in the water (difference between the ozone concentration at interface, ozone solubility, and dissolved ozone concentration in the water bulk). Consequently, in most kinetic models, the rate of ozone absorption equals the physical absorption rate. While this approach can be taken as correct when the chemical reaction rate is equal to the mass transfer rate, it does not hold when ozone is mainly con-

\* Corresponding author.

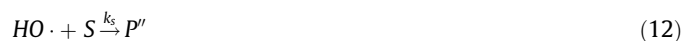
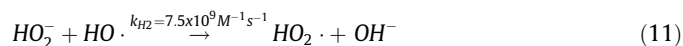
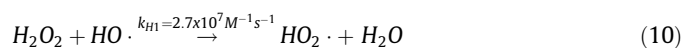
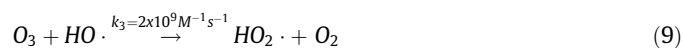
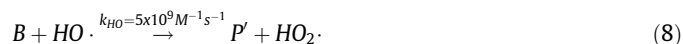
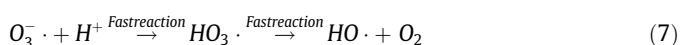
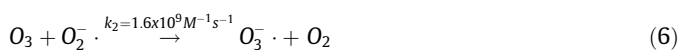
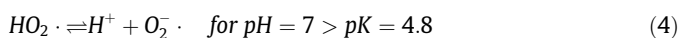
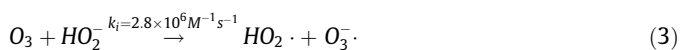
E-mail address: [fjrvivas@unex.es](mailto:fjrvivas@unex.es) (F.J. Rivas).

sumed in the proximity of the gas water interface, that is, when dealing with fast or moderate ozone reactions [17]. Under fast moderate ozone reaction regimes, ozone absorption rate is much higher than the simple physical absorption rate. Accordingly, the proposed kinetic model lacks sufficient accuracy. The parameter that measures the increase of ozone absorption rate (gas absorption, in general) when the reacting dissolved ozone undergoes reactions in the proximity of the interface, a distance from the water bulk called film layer, is the enhancement or reaction factor, E [18,19]. In general, this factor is usually taken as unity in most kinetic models. However, depending on the relative importance of mass transfer and chemical reaction rates, E can reach higher values. In the latter cases, the actual ozone absorption rate is clearly underestimated. Literature only reports a few studies considering the effect of direct ozone reactions in the film layer, although these studies do not consider the possibility that film free radical reactions can also affect the process rate or the reaction factor. The first work treating this subject was due to Benbelkacem and Debellefontaine [20], their study focusing on ozone direct reactions without formation of free radicals was just centered in the case of maleic or fumaric direct ozonation reactions. Also, in a more recent work Chavez et al. [21] have shown the importance of ozone direct reactions in the proximity of the interface considering the simultaneous direct reactions of ozone and antibiotics. However, free radicals can also be generated in the film layer where they can also react with organics and ozone. The potential formation of free radicals in the film layer is another aspect that literature has not yet considered. Then, formation of free radicals in the film when the reaction factor is higher than unity is normally neglected. This can also underestimate the reaction factor, and the removal rate of compounds that react with ozone.

In this work, a theoretical study on the importance of ozone reactions, (including free radical reactions), in the proximity of gas–water interface and how the formation of hydroxyl radicals in this liquid zone affects the reaction factor, is completed. This study is based on the application of gas-absorption theories, (film and penetration theories). The effect of mass transfer and chemical reactions is assessed by means of the analysis of mass transfer coefficient and direct rate constant influence. Additionally, the effect of the initial concentrations of generic compound B and hydrogen peroxide on the concentration profiles of reactants and hydroxyl radicals in the film layer and time is also studied.

### The reaction system

The following set of reactions have been considered to study the effects of the presence of hydroxyl radicals in a fast-moderate ozone reaction with a given compound B [22]:



In this reaction system, P, P' and P'' are byproducts that can also undergo oxidation reactions; however, these reactions are not considered in this study. Direct reaction (1) of ozone with B is a typical reaction of ozone processes when B is an ozone fast reacting compound. This scenario occurs when, for instance, the B molecule contains carbon double bonds or aromatic rings with activating groups. In a number of ozone direct reactions, hydrogen peroxide is generated. Hydrogen peroxide can thereafter react with ozone initiating a free radical mechanism, leading to the formation of hydroxyl radicals. Additionally, these free radicals can also react with the target compound B, that is, the so-called indirect reaction of B. Examples of these compounds can be some antibiotics or polynuclear aromatics [23,24]. For instance, ozone attacks resorcinol (ortho-dihydroxybenzene) in a 1,3 dipolar cycloaddition reaction to form an ozonide compound that decomposes. In the process, the aromatic ring is broken releasing hydrogen peroxide. Once hydrogen peroxide is in the medium, its ionic form (hydroperoxide ion,  $HO_2^-$ ) reacts with ozone to form free radicals through reaction (3). The latter stage is the main initiation reaction of the free radical mechanism. Hydrogen peroxide can also be generated from the self-decomposition of ozone catalyzed by hydroxyl anions (reaction (5)). However, the contribution of this reaction is commonly negligible because of its low-rate constant, especially at  $pH < 8$ . In any case, in this study, a constant  $pH \geq 6$  is considered so that equilibrium (4) is totally shifted to the right to form the superoxide ion radical ( $O_2^- \cdot$ ). This means that in any reaction where the hydroperoxide radical ( $HO_2 \cdot$ ) is formed (reactions (3), (8) and (9) to (11)), the immediate formation of the superoxide ion radical proceeds. Therefore, the decomposition rates of  $HO_2 \cdot$  through the aforementioned reactions are, in fact, formation rates of  $O_2^- \cdot$ . The free radical mechanism usually ends with termination reaction (12) because of the presence of hydroxyl radical scavengers, S. According to this mechanism, reaction rates of dissolved ozone, B, total  $H_2O_2$  and hydroxyl and superoxide ion radicals are as follows:

For dissolved ozone:

$$-r_{O_3} = [k_D C_B + k_1 10^{pH-14} + k_i A C_{HT} + k_2 C_{O_2r} + k_3 C_{HOR}] C_{O_3} \quad (13)$$

where  $C_{HT}$  is the total concentration of hydrogen peroxide (sum of concentrations of its ionic and non-ionic forms), A the fraction of the ionic form of hydrogen peroxide, defined as:

$$A = \frac{10^{pH-pK_H}}{1 + 10^{pH-pK_H}} \quad (14)$$

and  $C_{O_3}$ ,  $C_B$ ,  $C_{O_2r}$  and  $C_{HOR}$ , the concentrations of dissolved ozone, compound B, and superoxide ion and hydroxyl radicals, respectively. Also,  $10^{pH-14}$  is the concentration of the hydroxyl anion.

For B:

$$-r_B = [z k_D C_{O_3} + k_{HO} C_{HOR}] C_B \quad (15)$$

where z is the stoichiometric ratio of the ozone-B reaction (moles of B consumed per mol of ozone consumed).

For total hydrogen peroxide:

$$-r_{HT} = [k_i AC_{O_3} + k_H C_{HO} - k_1 C_{O_3} 10^{pH-14} - k_D C_{O_3} C_B] C_{HT} \quad (16)$$

where  $k_H$  is the global reaction rate constant involving reactions (10) and (11):

$$k_H = \frac{k_{H1} + k_{H2} 10^{pH-pK_H}}{1 + 10^{pH-pK_H}} \quad (17)$$

For hydroxyl radical:

$$-r_{HOR} = [k_{HO} C_B + k_3 C_{O_3} + k_H C_{HT} + k_T] C_{HOR} - [k_i AC_{HT} - k_2 C_{O_2r}] C_{O_3} \quad (18)$$

where  $k_T$  is the product between the concentration of hydroxyl radical scavengers,  $C_s$ , and their rate constant of their reaction with these free radicals,  $k_s$  (reaction (12)).

For superoxide ion radical:

$$-r_{O_2r} = k_2 C_{O_3} C_{O_2r} - [k_i AC_{HT} + k_3 C_{HOR}] C_{O_3} - [k_H C_{HT} + k_{HO} C_B] C_{HOR} \quad (19)$$

### The reaction factor

According to the film theory [25] when a reacting gas, like ozone, is being absorbed in a liquid (water in this case) it can react in a film layer close to the gas–liquid interface and/or in the water bulk. When ozone reactions are fast or moderate [17], all or a fraction of dissolved gas reacts in the film, a fact which is not usually considered when modeling ozonation systems [21]. In fact, as far as these authors know, no work has already been published considering the simultaneous presence of direct and indirect (free radical) ozone fast or moderate reactions in the film. Only the case of direct ozone reactions in the film has been considered [20,21]. Thus, with some exceptions, in most of ozonation processes, and regardless of the presence of reactions in the film, the ozone absorption rate is considered as the ozone mass transfer to the water through the film, that is:

$$N_{O_3} = k_L a (C_{eq} - C_{O_3}) = r_{O_3} \quad (20)$$

where  $k_L a$  is the volumetric mass transfer coefficient that for bubble columns or agitated tanks can take values between  $3 \times 10^{-3}$  and  $0.5 \text{ s}^{-1}$  [17] and  $C_{eq}$  is the ozone solubility or equilibrium dissolved ozone concentration at the gas–water interface.  $C_{eq}$  can be known from the ozone partial pressure,  $P_{O_3}$ , and Henry's law constant,  $He$  [26]:

$$C_{eq} = \frac{P_{O_3}}{He} = \frac{C_{O_3g} RT}{He} \quad (21)$$

where  $C_{O_3g}$ ,  $R$  and  $T$  are the concentration of ozone in the gas leaving the reactor (in equilibrium with  $C_{eq}$ ), the perfect gas constant and temperature, respectively.

However, when reactions occur in the film, equation (20) does not hold. In these cases, the ozone absorption rate is increased due to the presence of these fast-moderate reactions. In this scenario, the dimensionless reaction factor number is defined:

$$E = \frac{N_{O_3}}{k_L a (C_{eq} - C_{O_3})} \quad (22)$$

$E$  represents the number of times the physical ozone absorption rate is increased due to fast-moderate reactions in the film. It is evident that neglecting the effect of ozone film reactions implies that  $E = 1$ .

Now, in this work  $E$  values corresponding to the ozone process constituted by reactions (1) to (12) have been calculated under different conditions and compared to the case where no film (direct and free radical) reactions take place in the film layer. In any case,

$N_{O_3}$  can be determined from the application of Fick's law at the gas–water interface:

$$N_{O_3} = -D_{O_3} a \left. \frac{dC_{O_3}}{dx} \right|_{x=0} \quad (23)$$

where  $x = 0$  means interfacial conditions,  $D_{O_3}$  is the ozone diffusivity in water ( $1.3 \times 10^{-9} \text{ m}^2 \text{ s}^{-1}$  at  $25^\circ \text{C}$ , [27]) and the parameter "a" is the specific interfacial area. Solving equation (23) requires the ozone concentration profile through the film to be known. Film concentration profiles of species constituting the mechanism studied can also be used to compare the importance of free radical reactions. According to film theory [21,28] these profiles can be determined by solving the reaction–diffusion equations of species through the film layer. These equations are of the type:

$$D_j \frac{d^2 C_j}{dx^2} + r_j = 0 \quad (24)$$

where subindex  $j$  refers to any compound of the studied mechanism (dissolved ozone, B, etc.) and  $D_j$  its corresponding diffusivity in water. Boundary conditions needed to solve the mathematical model are:

$$\text{At } x = 0 \quad C_{O_3} = C_{eq} \quad \text{and} \quad \left. \frac{dC_i}{dx} \right|_{x=0} = 0 \quad (25)$$

where  $i$  means any other species but ozone that is not a volatile compound, and

$$\text{At } x = \delta \quad C_i = C_{i0} \quad \text{and} \quad -D_{O_3} a \left. \frac{dC_{O_3}}{dx} \right|_{x=\delta} = -r_{O_3} (\beta - a\delta) \quad (26)$$

where  $\delta$  is the film width. According to film theory,  $\delta$  is the ratio between ozone diffusivity and the individual liquid side mass transfer coefficient:  $D_{O_3}/k_L$ . For a typical  $k_L$  value of  $5 \times 10^{-5} \text{ ms}^{-1}$ , at  $25^\circ \text{C}$ ,  $\delta = 26 \text{ }\mu\text{m}$ . Also,  $\beta$  is the liquid hold-up in the reactor and subindex  $x=\delta$  means conditions at the film–water bulk interface.

More details of the mathematical model, that, hereinafter, will be named kinetic model 1, are given in the Supplementary section. The system was solved with the `bvp5c` Matlab solver at different values of  $k_D$ ,  $k_L$ ,  $C_B$ ,  $pH$  and  $C_{HT}$ . These parameters are considered the main variables that may influence the mass transport and reaction in the film layer (see also Supplementary part for dimensionless equations). Solution of kinetic model 1 requires a value different than zero for the concentration of ozone gas leaving the reactor at the start of the process,  $C_{O_3g}$ . To overcome this problem, a first value of  $10^{-11} \text{ M}$  was taken. This is significantly low, but this value allowed the calculation of the ozone solubility ( $C_{eq}$ ) at the gas–water interface after application of perfect gas and Henry laws (equation (21)). However, as revealed below, most of solutions of the kinetic model 1 were obtained by calculating  $C_{O_3g}$  as the logarithmic mean of an assumed  $C_{O_3g-outlet} = 10^{-11} \text{ M}$  (at the reactor outlet) and ozone concentration in the inlet gas,  $C_{O_3g-inlet}$  ( $2 \times 10^{-4} \text{ M}$ ):

$$C_{O_3g} = \frac{C_{O_3g-inlet} - C_{O_3g}}{\ln \frac{C_{O_3g-inlet}}{C_{O_3g}}} \quad (27)$$

The reason for this change was to show a higher variability of results for the concentration of B within the film.

## Results and discussion

As indicated above, kinetic model 1 was first solved starting with  $C_{O_3g} = 10^{-11} \text{ M}$  at the gas–water interface. Some results of the changes of ozone and B concentration within the film dimensionless layer ( $\alpha$ ) are shown in Fig. 1. As it is seen, in all cases, concentration of B does not change within the film layer as a result of the low ratio between diffusion rates of B and ozone (see  $E_i-1$  in

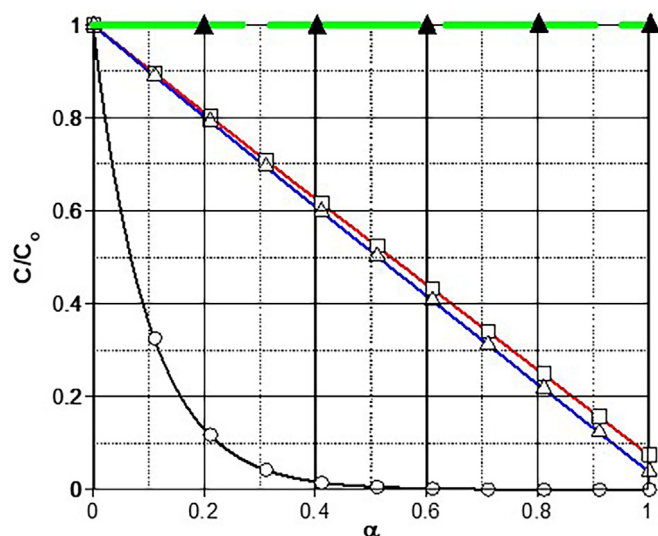


**Fig. 1.** Changes of calculated dimensionless concentration of ozone (open symbols) and generic compound B (solid symbols) within the film layer. Main conditions:  $\circ$ :  $k_D = 10^6 \text{ M}^{-1}\text{s}^{-1}$ ,  $C_{B0} = 2 \times 10^{-4} \text{ M}$ ;  $\triangle$ :  $k_D = 10^3 \text{ M}^{-1}\text{s}^{-1}$ ,  $C_{B0} = 2 \times 10^{-4} \text{ M}$ ;  $\square$ :  $k_D = 10^6 \text{ M}^{-1}\text{s}^{-1}$ ,  $C_{B0} = 10^{-7} \text{ M}$ .  $\blacktriangle$ : Valid for the three cases. Other general conditions shown in bottom of Table 1.

Table 1). The results of Fig. 1 correspond to cases of a fast pseudo first order reaction, moderate reaction, and slow reaction (see also Table 1 for representative dimensionless parameter values of Eqs. (28) and (29):  $Ha$  and  $E_i$ , respectively). In order to study cases with variability in the concentration profile of B,  $C_{O_{3g}}$  was changed as commented in section 1. The new value can be representative of the situation after some seconds from the start of ozonation so that it can also be taken as a good approximation.

### Influence of variables

Variables affecting the reaction factor due to diffusion and reaction in the film, for a given reacting gas (ozone in this case), are

**Table 1**  
Conditions of main variables, calculated reaction factor and  $E_i$ -1 and Hatta numbers.<sup>a</sup>

$k_D, \text{M}^{-1}\text{s}^{-1}$	$k_L, \text{ms}^{-1}$	$C_{B0}, \text{M}$	pH	$C_{HT}, \text{M}$	Ha	$E_i$ -1	E			
$10^7$	$5 \times 10^{-5}$	$2 \times 10^{-4}$	7	0	32	44.5	23			
$10^6$					10.2		9.2			
$10^5$					3.2		3.2			
$10^4$					1.0		1.3			
$10^3$					0.3		1.03			
$10^2$					0.1		1.02			
10					0.03		1.0			
$10^6$					$4 \times 10^{-4}$		1.3	1.5		
					$5 \times 10^{-5}$		$2 \times 10^{-5}$	3.2	54.5	2.6
							$2 \times 10^{-6}$	1.02	0.44	1.2
		$10^{-7}$	0.23	0.02	1.01					
		$10^{-10}$	0.007	1	1					
		$2 \times 10^{-4}$	10	10.2	48.1	9.3				
			10	$10^{-2}$	10.2	42.6	9.2			
			10	$10^{-2}$	10.2	48.1	9.3			
$10^5$			10	$10^{-2}$	3.2	48.1	3.2			
			10	$10^{-2}$	0.34	4.0	1.0			
$10^6$	$1.5 \times 10^{-4}$	$2 \times 10^{-5}$	10	$10^{-2}$	1.1	44.4	1.3			
$10^5$	$5 \times 10^{-5}$	$2 \times 10^{-4}$	10	$10^{-2}$	3.2	48.1	3.2			
$10^{6b}$					10.2		9.2			
$10^{6c}$					10.2		9.2			
$10^{6d}$					10.2		9.2			
$10^{6e}$					10.2		10.2			
$10^{3f}$					0.32		$5.3 \times 10^7$	10.2		
$10^{6g}$					0.23		$5.3 \times 10^7$	10.4		
							$2.6 \times 10^4$	1.0		

<sup>a</sup> Results at the start of reactions assuming  $C_{O_{3ge}} = 2 \times 10^{-4} \text{ M}$  ( $C_{eq} = 2.4 \times 10^{-6} \text{ M}$ ) and  $z = 1$ . Other general conditions applied unless indicated:  $k_{La} = 8 \times 10^{-3} \text{ s}^{-1}$ ,  $\beta = 0.9$ ,  $k_T = 0$ ,  $v_g = 20 \text{ Lh}^{-1}$ ,  $k_{La} = 4 \times 10^{-2} \text{ s}^{-1}$ ,  $\beta = 0.7$ ,  $k_T = 10^4 \text{ s}^{-1}$ ,  $C_{O_{3g}} = 10^{-11} \text{ M}$  ( $C_{eq} = 2.0 \times 10^{-12} \text{ M}$ ),  $C_{O_{3g}} = 10^{-11} \text{ M}$  ( $C_{eq} = 2.0 \times 10^{-12} \text{ M}$ ) and  $k_D = 10^3 \text{ M}^{-1}\text{s}^{-1}$ ,  $C_{O_{3g}} = 10^{-11} \text{ M}$  ( $C_{eq} = 2.0 \times 10^{-12} \text{ M}$ ) and  $C_{B0} = 10^{-7} \text{ M}$ .

present in the dimensionless numbers of Hatta,  $Ha$ , and instantaneous reaction factor,  $E_i$ :

$$Ha = \frac{\sqrt{k_D D_{O_3} C_B}}{k_L} \quad (28)$$

and

$$E_i - 1 = \frac{D_B C_B}{z D_{O_3} C_{eq}} \quad (29)$$

where  $D_B$  stands for the diffusivity of B in water. While  $Ha$  represents the relative importance of chemical and physical absorption rates in the film layer,  $E_i - 1$  is an estimation of the diffusion transport ratio between B and ozone through the film layer. The rate constant of the ozone-B direct reaction,  $k_D$ , the liquid phase mass transfer coefficient,  $k_L$ , the ratio of diffusivities in water,  $D_B/D_{O_3}$ , the equilibrium concentration of ozone, and concentration of compound B, are the variables and/or properties that influence the diffusion and reaction rates through the film layer. It should be highlighted that in the system constituted by reactions (1) to (12) there are five  $Ha$  numbers, corresponding to the reactions of ozone with B,  $\text{OH}^-$ ,  $\text{HO}_2^-$ , and hydroxyl and superoxide ion radicals (see Supplementary information). However, only the first one and  $E_i - 1$  will be indicative of any change of B concentration in the film layer as shown below. Because temperature is taken as 25 °C, ozone and B diffusivities will remain constant, and no effects of these properties are considered. Variables finally studied are  $k_D$ ,  $k_L$ ,  $C_{B0}$  (which affect  $Ha$  and  $E_i - 1$ ), pH and  $C_{HT}$ . On one hand, pH affects ozone solubility and formation of  $\text{HO}_2^-$  and, on the other hand, the presence of hydrogen peroxide triggers reaction (3), initiating the free radical reaction chain.

Table 1 shows some values of the variables tested, calculated values of corresponding reaction factor,  $E_i - 1$ , and Hatta of ozone reaction with B. In addition to main variables listed in Table 1, solution of the kinetic model 1 was also obtained at different  $k_{La}$ ,  $\beta$  and  $k_T$  that could also affect, although to a lesser extent, the reaction factor (see Table 1).

Conditions applied to variables are those commonly used in ozone processes [29]. The main conclusion deduced from Table 1 is that pH and/or initial hydrogen peroxide concentration, which according to the reaction mechanism, have an influence on free radical formation, do not affect or slightly affect the reaction factor, provided that the rest of main variables included in the Hatta number remain constant. Also, equal or similar values of  $E$  implies the similarity in the ozone absorption rate. For example, for generic conditions applied with  $k_D = 10^6 \text{ M}^{-1}\text{s}^{-1}$ ,  $E$  slightly increases from 9.22 to 9.34 when pH changes from 7 to 10, respectively. Additionally, keeping constant the  $\text{pH} = 7$ , an increase in the initial hydrogen peroxide concentration up to  $10^{-2} \text{ M}$  results in no change in  $E$  that practically remains constant at 9.23. Previous results suggest that free radical reactions, although present, do not affect the ozone absorption rate and likely the rate of B removal in the film layer. This hypothesis is also confirmed by two facts: on one hand, the values of  $E$  obtained by running the kinetic model 1 without free radical reaction contribution and, on the other hand, the observed dimensionless concentration profiles of ozone and B throughout the film layer (also without considering free radical reactions). In these cases,  $E$  values are practically coincident with those shown in Table 1. Moreover, concentration profiles through the film layer also coincide in both mechanisms.

#### Influence of $k_D$ , pH and $C_{HT}$

Figs. 2 and 3 show the effect of  $k_D$ , pH and total hydrogen peroxide concentration on the concentration profiles of ozone and  $C_B$  through the film layer, respectively. As observed, concentration profiles are deeply affected by the direct rate constant value  $k_D$ . In the case of ozone (Fig. 2), almost total consumption in the film layer is obtained when  $k_D$  is higher than  $10^3 \text{ M}^{-1}\text{s}^{-1}$ . Under these conditions ( $k_D > 10^3 \text{ M}^{-1}\text{s}^{-1}$ )  $Ha$  values are higher than 0.3 (moderate-fast reaction regime). On the contrary, lower values of  $k_D$  leading to  $Ha \leq 0.3$  (slow reaction regime) involve that significant amounts of ozone reach the water bulk (at  $\alpha = 1$ ). These results are in accordance to those expected taking into account the  $Ha$  value [17]. Similar ozone concentration profiles are obtained if pH is increased to 10 and/or hydrogen peroxide is added.

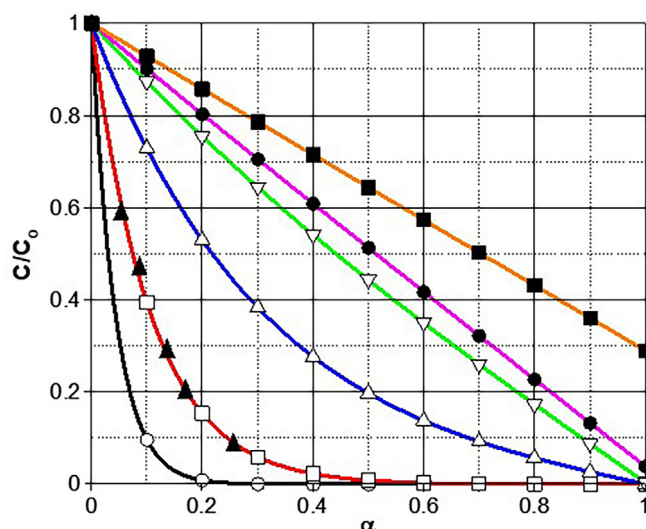


Fig. 2. Changes of calculated dimensionless concentration of ozone through the film layer at different  $k_D$ . Conditions: pH 7,  $k_D$ ,  $\text{M}^{-1}\text{s}^{-1}$ : ■:  $10^2$ , ●:  $10^3$ , ▽:  $10^4$ , △:  $10^5$ , □:  $10^6$ , ○:  $10^7$ . ▲: pH 10 with and without  $10^{-2} \text{ M H}_2\text{O}_2$  and  $k_D = 10^6 \text{ M}^{-1}\text{s}^{-1}$ . Other conditions are shown at the bottom of Table 1.

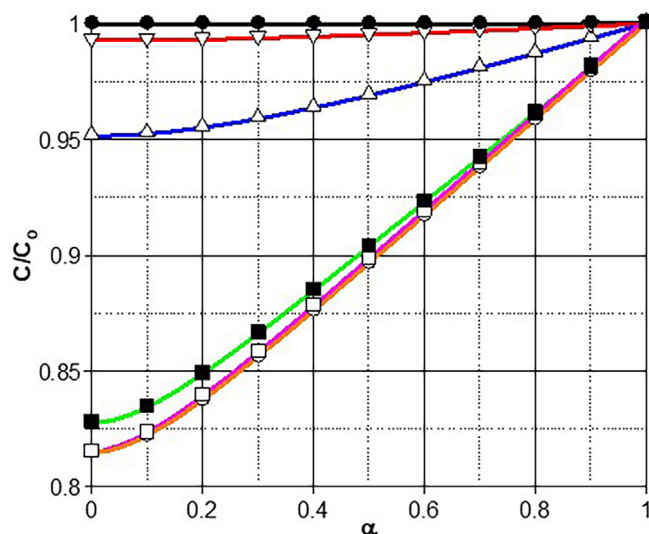


Fig. 3. Changes of calculated dimensionless concentration of generic compound B through the film layer at different  $k_D$ , pH and  $C_{HT}$ . General conditions unless indicated: pH 7,  $k_D$ ,  $\text{M}^{-1}\text{s}^{-1}$ : ●:  $10^2$ , ▽:  $10^4$ , △:  $10^5$ , ○:  $10^6$ , □:  $k_D = 10^6 \text{ M}^{-1}\text{s}^{-1}$ , pH 10, ■:  $k_D = 10^6 \text{ M}^{-1}\text{s}^{-1}$ , pH 10,  $10^{-2} \text{ M H}_2\text{O}_2$ . Other general conditions are shown at the bottom of Table 1.

The negligible contribution of the free radical reaction (8) to remove B is undoubtedly due to the low concentration of hydroxyl radicals. In other words, removal rate of B is practically due to the ozone direct reaction in the film. These results are also experienced when other  $k_D$  values leading to  $Ha > 0.3$  are tested (that is, for fast-moderate direct ozone-B reactions). Lower values of  $k_D$  involving  $Ha < 0.3$ , imply the negligible reaction in the film (dimensionless ozone concentration drop is only due to diffusion transfer).

Changes of dimensionless concentration of B in the film layer (see Fig. 3), keeping approximately constant  $E_{i-1}$  (see Table 1), confirm the results deduced from Fig. 2 for dissolved ozone concentration. Direct reaction of ozone-B is essentially the only responsible step for the removal of B, with negligible contributions of free radical reaction (8) when  $k_D > 10^2 \text{ M}^{-1}\text{s}^{-1}$ , that is, for fast-moderate kinetic regimes. However, at pH 10 with  $C_{HT} = 10^{-2} \text{ M}$  drop of B concentration within the film layer is slightly lower than in the absence of added  $\text{H}_2\text{O}_2$ . As it will be shown later, this is mainly due to competition of reaction (3) with reaction (1). Reaction (8) has negligible influence.

Figs. 4 and 5 show the changes of calculated concentrations of total hydrogen peroxide and hydroxyl radicals in the film layer, respectively. Fig. 4 reveals that raising  $k_D$  leads to significant increases of hydrogen peroxide concentration due to its formation in the ozone-B direct reaction. However, it is also noticed that increasing the pH from 7 to 10 results in a small decrease of hydrogen peroxide concentration. The latter finding is likely due to  $\text{H}_2\text{O}_2$  consumption with hydroxyl radicals. In this sense, it has to be pointed out that the global rate constant,  $k_H$  (equation (17)) is pH dependent. In any case, the presence of hydroxyl radicals at the calculated concentrations has no influence on the removal of B. In Fig. 5, the calculated changes of hydroxyl radical concentration within the film layer are shown. It is seen that increasing  $k_D$  and/or pH leads to an increase in  $\text{HO}^\cdot$  concentration. However, it is also observed a significant decrease of  $\text{HO}^\cdot$  concentration, when hydrogen peroxide ( $0.01 \text{ M}$ ) is added (pH 10). This means that hydrogen peroxide mostly consumes the free radicals, which are not available to remove B through reaction (8).

In Figure S1 the effect of adding hydrogen peroxide keeping constant the rest of variables and properties is shown. Hydrogen peroxide concentration diminishes from water bulk to the gas-wa-

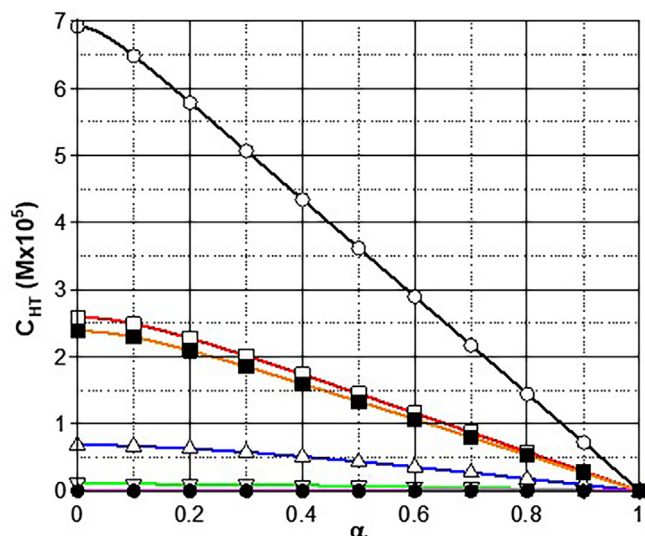


Fig. 4. Changes of calculated total hydrogen peroxide concentration through the film layer at different  $k_D$ . Conditions: pH 7,  $k_D = 10^6 \text{ M}^{-1}\text{s}^{-1}$ ;  $\bullet$ ,  $10^2$ ,  $\nabla$ ,  $10^4$ ,  $\triangle$ ,  $10^5$ ,  $\square$ ,  $10^6$ ,  $\circ$ :  $10^7$ ,  $\blacksquare$ : pH 10 and  $k_D = 10^6 \text{ M}^{-1}\text{s}^{-1}$ . Other general conditions are shown at the bottom of Table 1.

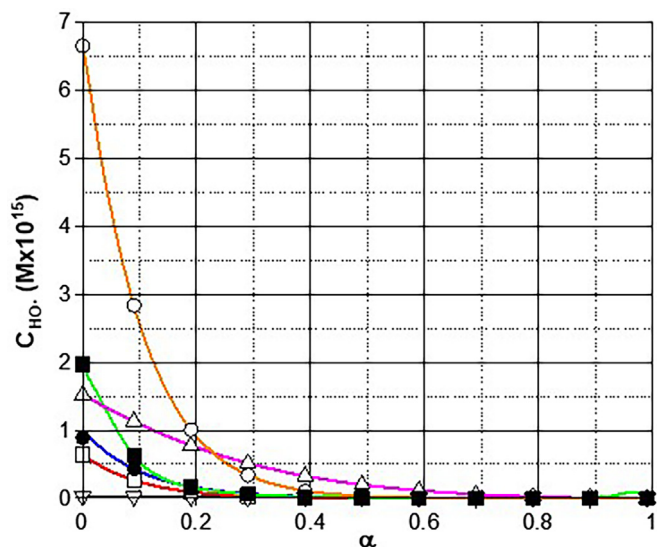


Fig. 5. Changes of calculated hydroxyl radical concentration through the film layer at different  $k_D$ , pH and  $C_{HT}$ . Conditions: pH 7,  $k_D = 10^3$ ,  $\triangle$ ,  $10^5$ ,  $\circ$ ,  $10^6$ ,  $\square$ : pH 6 and  $k_D = 10^6$ ,  $\blacksquare$ : pH 10,  $C_{H_2O_2} = 10^{-4} \text{ M}$  and  $k_D = 10^6$ ,  $\bullet$ : pH 10,  $C_{H_2O_2} = 0.01 \text{ M}$  and  $k_D = 10^6$ . Other general conditions are shown at the bottom of Table 1.

ter interface because of the reaction with hydroxyl radicals. This means that this reaction is more important than its formation through the direct ozone-B reaction. It is also inferred that the increase of pH leads to a faster consumption of hydrogen peroxide due to reactions (3) and (11). Additionally, hydrogen peroxide concentration increases when it is not initially present because of the direct ozone-B reaction. However, in any case, these results have negligible influence on the removal rate of B.

*Influence of  $k_L$*

Similarly to the influence of  $k_D$ , the liquid side mass transfer coefficient,  $k_L$ , also affects the Hatta number and, as a consequence, ozone and B concentration profiles. Fig. 6 displays the changes of

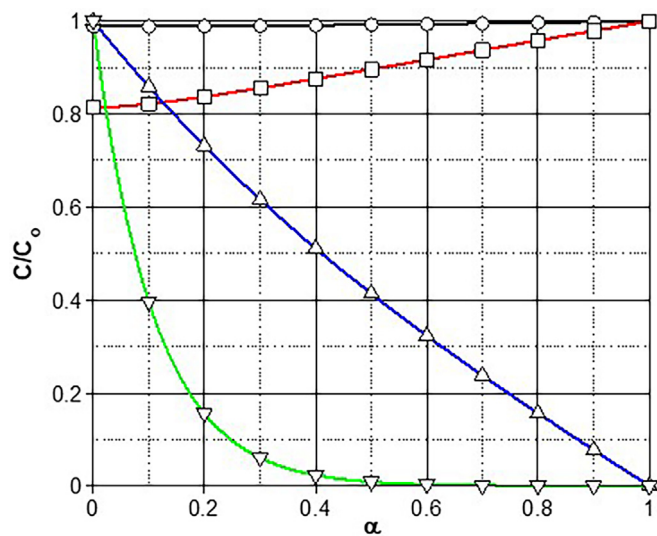


Fig. 6. Changes of calculated dimensionless concentration of ozone and generic compound B through the film layer at different  $k_L$ . Conditions: pH 7,  $k_D = 10^6 \text{ M}^{-1}\text{s}^{-1}$ ,  $C_{B0} = 2 \times 10^{-4} \text{ M}$  and others as shown at the bottom of Table 1.  $k_L$ ,  $\text{ms}^{-1} = 5 \times 10^{-5}$ ;  $\nabla$ ,  $\text{O}_3$ ,  $\square$ , Compound B.  $k_L$ ,  $\text{ms}^{-1} = 410^{-4}$ ;  $\triangle$ ,  $\text{O}_3$ ,  $\circ$ , Compound B.

ozone and B dimensionless concentrations through the film layer for two values of  $k_L$ .

As observed, if compared to  $k_D$  influence,  $k_L$  has the opposite effect on ozone and B concentration profiles. An increase of  $k_L$  leads to a decrease of ozone and B concentration drops. With  $k_L = 4 \times 10^{-4} \text{ s}^{-1}$ ,  $Ha$  is 1.2, which involves the development of moderate regime. The progress of moderate regimes agrees with the shape of the ozone curve shown in Fig. 6 corresponding to the case where ozone drop concentration is nearly due to mass transfer diffusion. Also, drop of B concentration is negligible due to moderate transport and reaction in the film. Previous results contrast with the shape of the curves with  $k_L = 5 \times 10^{-5} \text{ ms}^{-1}$ . In this case the kinetic regime corresponds to fast regime (fast simultaneous diffusion and reaction). In any case, no influence of free radical reactions was observed on these concentration profiles when kinetic model 1 was solved without the contribution of free radical reactions.

*Influence of  $C_{B0}$*

In Fig. 7 the changes of dimensionless concentration of ozone and B within the film layer are shown for different initial concentrations of B in the water bulk. Since concentration of B positively affects both the Hatta number and  $E_i-1$ , drops of concentrations of B increase with decreasing  $C_{B0}$  (or  $E_i-1$ ) while ozone concentrations drop decrease. Thus, for  $C_{B0} = 10^{-10} \text{ M}$ , ozone concentration drop is negligible which means that at these conditions the diffusion rate of ozone is much higher than that of B and there is negligible reaction in the film as well (chemical regime very slow reaction). The drop of B concentration observed is undoubtedly due to the very low value of the ratio between diffusion rates of B and ozone (about  $10^{-4}$  or  $E_i-1 \approx 0$ ). In summary, the quantitative decrease of  $C_B$  concentration within the film layer is negligible because of the very low  $Ha$  number at these conditions. An opposite situation is observed for  $C_{B0} = 2 \times 10^{-4} \text{ M}$ . In this case, the reaction is fast ( $Ha > 3$ ) leading to a high ozone concentration drop but lower drop concentration of B because the ratio of diffusion rates of B and ozone (or  $E_i-1$ ) has increased about six orders of magnitude.

Fig. 8 shows the effect of  $C_{B0}$  on the formation of hydrogen peroxide. It is seen that hydrogen peroxide is formed at the film-water bulk interface and then slowly increases up to reach the gas-water

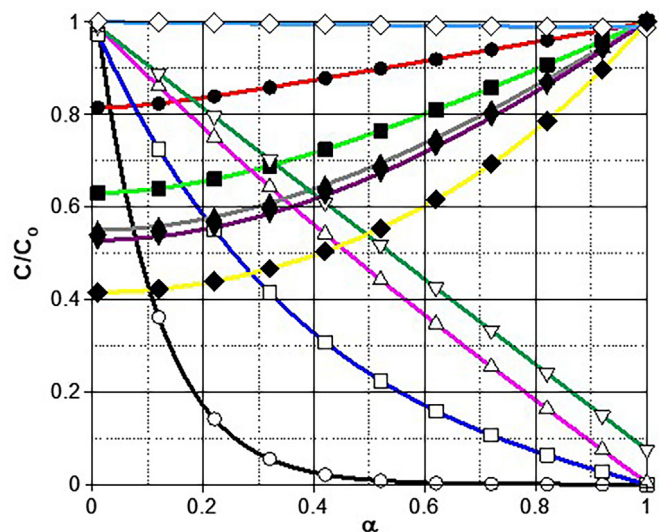


**Fig. 7.** Changes of calculated dimensionless concentration of ozone (open symbols) and generic compound B (solid symbols) through the film layer at different  $C_{B0}$ . Conditions: pH 7,  $k_D = 10^6 \text{ M}^{-1}\text{s}^{-1}$ ,  $k_L = 5 \times 10^{-5} \text{ M}$  and others as shown at the bottom of Table 1.  $C_{B0}$ , M:  $\bullet$ ,  $2 \times 10^{-4}$ ;  $\blacksquare$ ,  $2 \times 10^{-5}$ ;  $\blacktriangle$ ,  $2 \times 10^{-6}$ ;  $\blacktriangledown$ ,  $10^{-7}$ ;  $\blacklozenge$ ,  $10^{-10}$ .

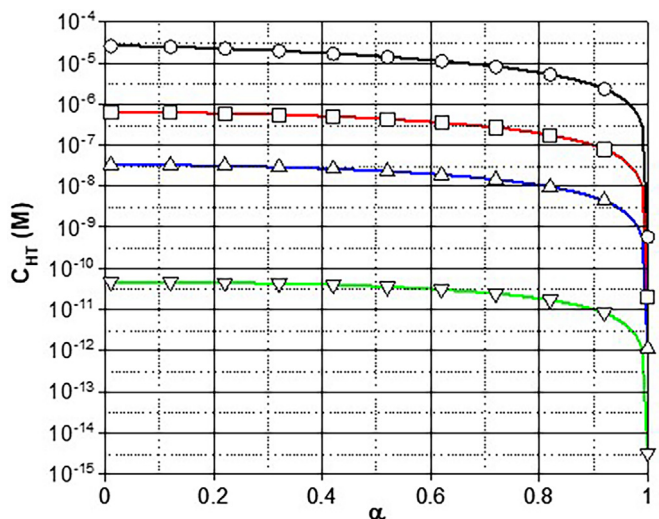


**Fig. 8.** Changes of calculated concentration of total hydrogen peroxide through the film layer at different  $C_{B0}$ . Conditions: pH 7,  $k_D = 10^6 \text{ M}^{-1}\text{s}^{-1}$ ,  $k_L = 5 \times 10^{-5} \text{ M}$  and others as shown at the bottom of Table 1.  $C_{B0}$ , M:  $\circ$ ,  $2 \times 10^{-4}$ ;  $\square$ ,  $2 \times 10^{-6}$ ;  $\triangle$ ,  $10^{-7}$ ;  $\nabla$ ,  $10^{-10}$ .

interface with concentrations raising with the increase of  $C_{B0}$ . However, the concentration of hydrogen peroxide formed mainly affects the formation of hydroxyl radicals (see also Fig. 9) since no effect on B concentration was observed when solving kinetic model 1 in the absence of free radical reactions.

In Fig. 9, hydroxyl radical concentration profiles within the film layer are shown calculated at different  $C_{B0}$  values. As expected, hydroxyl radical concentrations are too low ( $< 2 \times 10^{-14} \text{ M}$ ) to have an incidence on the removal of B at the start of reactions. In this case, the concentration of hydroxyl radical also increases from the water bulk interface to the gas–water interface but not with the increasing bulk concentration of B. It is also seen that for  $C_{B0} = 2 \times 10^{-4} \text{ M}$  hydroxyl radical concentration is lower than that calculated with  $C_{B0} = 2 \times 10^{-6} \text{ M}$ , which is undoubtedly due to reaction (8) though its contribution to remove B is negligible if compared to the direct reaction.

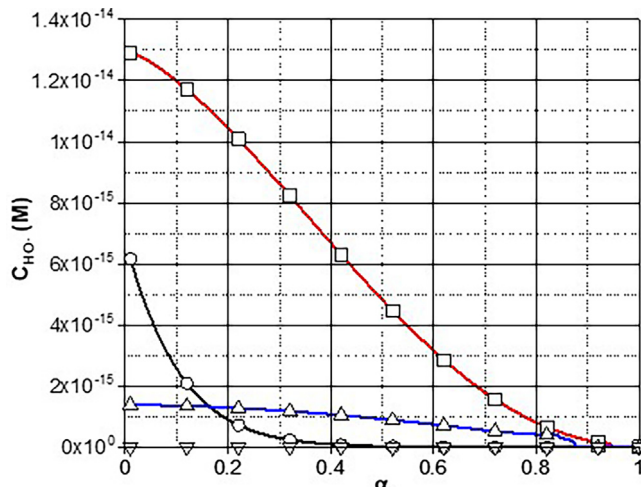


**Fig. 9.** Changes of calculated concentration of hydroxyl radical through the film layer at different  $C_{B0}$ . Conditions: pH 7,  $k_D = 10^6 \text{ M}^{-1}\text{s}^{-1}$ ,  $k_L = 5 \times 10^{-5} \text{ M}$  and others as shown at the bottom of Table 1.  $C_{B0}$ , M:  $\circ$ ,  $2 \times 10^{-4}$ ;  $\square$ ,  $2 \times 10^{-6}$ ;  $\triangle$ ,  $10^{-7}$ ;  $\nabla$ ,  $10^{-10}$ .

*Individual reaction rates*

The negligible effect of free radical reactions to remove B in the film layer can more easily be observed from the values of reaction rates of the mechanism steps as shown in Fig. 10. In Fig. 10 it is seen results of local reaction rates of ozone and hydroxyl radicals with B and hydrogen peroxide and also those of the reaction between ozone and hydroxyl radicals at three positions within the film layer ( $\alpha = 0, 0.5$  and 1) with  $k_D = 10^6 \text{ M}^{-1}\text{s}^{-1}$ ,  $C_{B0} = 2 \times 10^{-4} \text{ M}$  and pH 7. From Fig. 10, it is inferred that removal rates due to the direct reaction are always much higher than those of the hydroxyl radical-B reaction (indirect reaction). At gas–water and film water bulk interfaces, direct reaction is about  $10^5$  and  $10^7$  faster than the indirect reaction, respectively. Differences in reaction rates are always observed though with different importance at other conditions of  $k_D$ ,  $C_{B0}$ , pH, etc, which confirms the negligible contribution of free radical reactions to the ozonation of B (see also Figures S2 and S3). Direct reaction rates in the film layer are always higher than the indirect reaction rates regardless of the kinetic

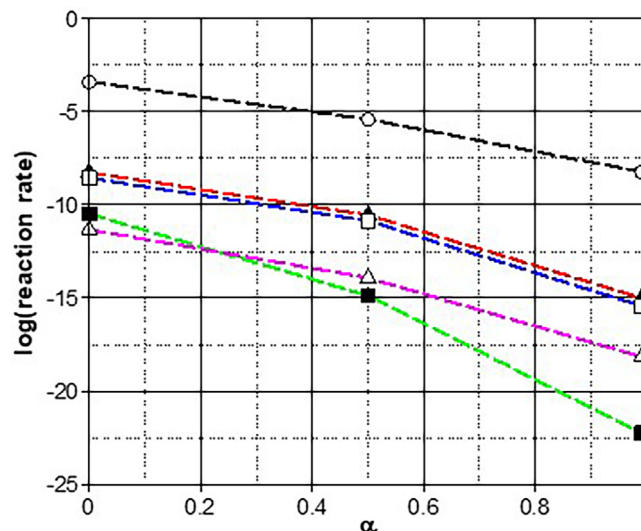


**Fig. 10.** Changes of main reaction rates within the film layer. General conditions shown at the bottom of Table 1.  $\circ$ : Direct Reaction (1),  $\blacktriangle$ : Indirect reaction (8),  $\square$ : Initiation reaction (3);  $\triangle$ : Ozone-HO reaction (9),  $\blacksquare$ : Hydrogen peroxide-HO reactions (10) and (11).

regime of ozonation (fast-moderate or even slow). It has to be noted that kinetic model 1 involving or not reactions in the film and water bulk do lead to different results as reported in a previous work but without considering the development of free radical reactions [21].

Results so far discussed refer to what happens in the film layer after a few seconds from the start of reaction but do not give bulk concentration profiles with time. Below, results of time bulk concentration profiles considering direct and free radical reactions in film and water bulk are also compared with the scenario where reactions in the film layer are not considered.

#### Time bulk concentration profiles

Bulk concentration profiles of the species studied with time with contributions of film and water bulk direct and free radical reactions (kinetic model 2) and only with water bulk direct and free radical reactions (kinetic model 3), have also been calculated. It should be highlighted that kinetic model 3 is the one usually applied in ozonation kinetic models in the literature [30]. Now, kinetic model 2 is constituted by dynamic diffusion–reaction mass balances according to renewal theories [31] combined with time mass balances of species present in bulk water. Kinetic model 3 is only formed by time mass balances of species in bulk water. Kinetic model 2, considering the ozonation is carried out in a perfectly stirred semibatch reactor, obeys the following equations:

Ozone mass balance in the gas phase:

$$\frac{dC_{O_3g}}{dt} = \frac{1}{V_T(1-\beta)} \left[ v_G C_{O_3ge} - v_G C_{O_3g} - EV_T k_i a \beta \left( C_{O_3g} \frac{RT}{He} - C_{O_3} \right) \right] \quad (30)$$

where  $v_G$ ,  $V_T$  are the gas flow rate and total reaction volume (gas plus water volume), respectively.

Ozone mass balance in water

$$\begin{aligned} \frac{dC_{O_3}}{dt} = & Dk_i a \left( C_{O_3g} \frac{RT}{He} - C_{O_3} \right) \\ & - \left[ C_{O_3} \left( k_D C_B + k_i A C_{HT} + k_2 C_{O_2r} + k_3 C_{HOR} + k_1 10^{pH-14} \right) \right] (\beta - a\delta) \end{aligned} \quad (31)$$

where  $D$  is the depletion factor [20] defined as follows:

$$D = \frac{-D_{O_3} a \left. \frac{dC_{O_3}}{dx} \right|_{x=\delta}}{k_i a (C_{eq} - C_{O_3})} \quad (32)$$

B mass balance

$$\frac{dC_B}{dt} = v_1 - C_B [k_D C_{O_3} + k_{HO} C_{HOR}] (\beta - a\delta) \quad (33)$$

Total hydrogen peroxide mass balance

$$\frac{dC_{HT}}{dt} = v_2 + \left[ k_1 10^{pH-14} C_{O_3} + k_D C_{O_3} C_B - C_{HT} (k_i A C_{O_3} + k_H C_{HOR}) \right] (\beta - a\delta) \quad (34)$$

Hydroxyl radical mass balance:

$$\begin{aligned} \frac{dC_{HOR}}{dt} = & v_3 + [(k_2 C_{O_2r} + k_i A C_{HT}) C_{O_3} - C_{HOR} (k_3 C_{O_3} \\ & + k_{HO} C_B + k_H C_{HT} + k_T)] (\beta - a\delta) \end{aligned} \quad (35)$$

Superoxide ion radical mass balance:

$$\begin{aligned} \frac{dC_{O_2r}}{dt} = & v_4 + [-k_2 C_{O_3} C_{O_2r} + C_{HOR} (k_H C_{HT} + k_3 C_{O_3} + k_{HO} C_B) \\ & + k_i A C_{O_3} C_{HT}] (\beta - a\delta) \end{aligned} \quad (36)$$

with  $v_1$ ,  $v_2$ ,  $v_3$  and  $v_4$  as the mol rates per volume of B, total hydrogen peroxide, hydroxyl radical and superoxide ion radical, respec-

tively, defined from Fick's law at the film–water bulk interface, in general form as:

$$v_i = -D_i a \left. \frac{dC_i}{dx} \right|_{x=\delta} \quad (37)$$

where subindex  $i$  represents any of the species mentioned above.

Initial boundary conditions of kinetic model 2 are:

$$t = 0 \quad C_i = C_{i0} \quad (38)$$

where  $C_{i0}$  is the concentration of species  $i$  at the start of reaction. In the case of ozone in the gas phase, a very low value of  $10^{-11}$  M was taken so that the kinetic model could be solved. For any reaction time, solution of mass balances requires to know the concentration of species at the film–bulk water interface. These concentrations were determined from the application of penetration theory [31]. This mass transport theory assumes a non-stationary situation in which liquid elements are exposed to the gas at the interface for a given time or renovation time,  $t_r$ , after which they are renewed by others coming from the water bulk. According to this theory, the diffusion–reaction mass balance of any species  $i$  through these elements is:

$$\frac{dC_i}{dt} = D_i \frac{\partial^2 C_i}{\partial x^2} + r_i \quad (39)$$

that can be solved with the initial and boundary conditions:

$$t = 0 \text{ (any } x \text{ value)} \quad C_i = C_{i0} \quad (40)$$

$$\begin{aligned} t > 0 \quad x = 0 \quad C_{O_3} = C_{eq} \quad \frac{dC_i}{dx} = 0 \\ x = \delta \quad C_i = C_{i0} \end{aligned} \quad (41)$$

For the case of ozone, in equation (40),  $C_{i0} = C_{O_30} = 0$  while in equations (41) at  $x = \delta$  and  $t > 0$ ,  $C_{i0}$  is the concentration of any species of the reacting system, ozone included.

Model 3 is just a simplification of model 2. The difference between both approaches is that in model 3,  $D = E = 1$  and  $v_i = 0$ , so equations 37 and 39–41 are not applied.

The *pdepe* Matlab solver was used to calculate concentration values at the waterbulk interface ( $x = \delta = 20 \mu\text{m}$ ). Thereafter, application of Fick's law, allowed the calculation of molar rates per volume of species being transported between film and water bulk,  $v_i$ , and the parameter  $D$ . Solver *pdepe* was simultaneously combined with the *ode23* Matlab routine to determine bulk concentration profiles (equations (30) to (36)). Equations (30) to (41) form kinetic model 2 where both direct and free radical reactions in film and water bulk are considered. To assess the incidence of film reactions, kinetic model 2 constituted by only direct and free radical reactions in the water bulk was also solved and identified as kinetic model 3. Also, kinetic model 2 was solved without the contributions of free radical reactions in the film (kinetic model 4). As an example, the influence of mainly  $k_D$  and  $C_{B0}$  when both kinetic models 2 and 3 are used is discussed herein. Results of the kinetic models 2 and 3 at different pH and total concentration of hydrogen peroxide are also discussed here but they are shown in the supplementary section (see Figures S9 and S10).

#### Influence of $k_D$

Results are shown in Figs. 11–15 and Figures S4.

In all cases, calculated concentrations of B from kinetic model 3 (without reactions in the film) are lower than those determined including all possible reactions both in the film and in water bulk (kinetic model 2). This means that the no inclusion of film reactions leads to overestimated concentrations of B. Differences in concentrations from both kinetic models 2 and 3 increase with the increase of  $k_D$ . For example, at 200 s and  $k_D = 10^6 \text{ M}^{-1}\text{s}^{-1}$  (fast



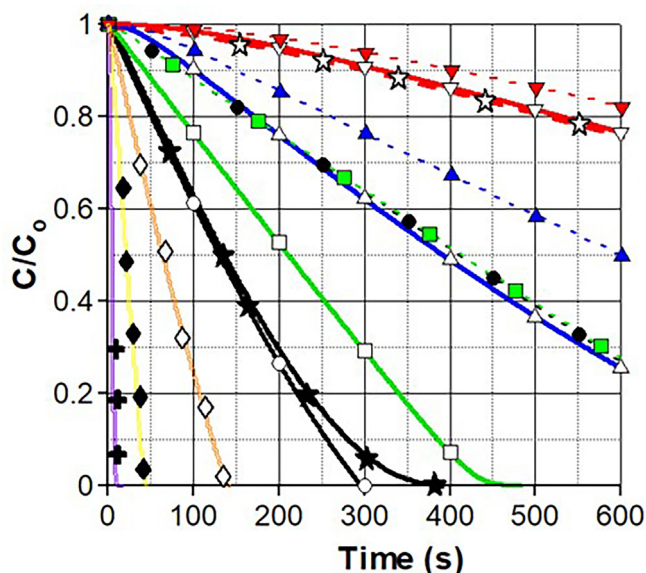


**Fig. 11.** Evolution of the normalized calculated profiles of a generic compound B during its ozonation in water. Conditions:  $C_{O_3\text{gin}} = 2 \times 10^{-4}$  M,  $\text{pH} = 7$ ,  $\beta = 0.98$ ,  $k_{l,a} = 2 \times 10^{-4} \text{ s}^{-1}$ ,  $k_l = 5 \times 10^{-5} \text{ m}^2 \text{ s}^{-1}$ ,  $V = 1.0 \text{ L}$ ,  $Q_g = 20 \text{ L h}^{-1}$ ,  $C_{B_0} = 2 \times 10^{-4}$  M. Direct rate constant ozone-B reaction,  $k_D$ :  $\bullet$  (black line),  $10^6 \text{ M}^{-1}\text{s}^{-1}$ ;  $\square$  (green line),  $10^4 \text{ M}^{-1}\text{s}^{-1}$ ;  $\triangle$  (blue line),  $10^2 \text{ M}^{-1}\text{s}^{-1}$ ;  $\nabla$  (red line),  $10 \text{ M}^{-1}\text{s}^{-1}$ . Open symbols: kinetic model 2. Solid symbols: kinetic model 3.  $*$ ,  $k_D = 10^6 \text{ M}^{-1}\text{s}^{-1}$  (kinetic model 4);  $\star$ ,  $k_D = 10 \text{ M}^{-1}\text{s}^{-1}$  (kinetic model 4). Influence of initial B concentration (kinetic model 2,  $k_D = 10^6 \text{ M}^{-1}\text{s}^{-1}$ ).  $C_{B_0} \times 10^5 \text{ M}$ :  $\diamond$ ; 8;  $\blacklozenge$ ; 2;  $\blackplus$ ; 0.2.

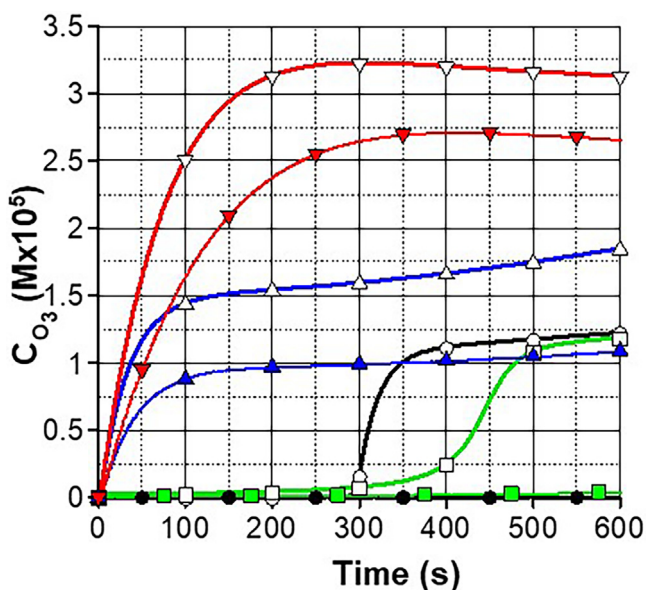


**Fig. 12.** Evolution of the dissolved ozone concentration in the ozonation of a generic compound (B). Conditions:  $C_{O_3\text{gin}} = 2 \times 10^{-4}$  M,  $\text{pH} = 7$ ,  $\beta = 0.98$ ,  $k_{l,a} = 2 \times 10^{-4} \text{ s}^{-1}$ ,  $k_l = 5 \times 10^{-5} \text{ m}^2 \text{ s}^{-1}$ ,  $V = 1.0 \text{ L}$ ,  $Q_g = 20 \text{ L h}^{-1}$ ,  $C_{B_0} = 2 \times 10^{-4}$  M. Direct rate constant ozone-B reaction,  $k_D \text{ M}^{-1}\text{s}^{-1}$ :  $\bullet$  (black line),  $10^6$ ;  $\square$  (green line),  $10^4$ ;  $\triangle$  (blue line),  $10^2$ ;  $\nabla$  (red line), 10. Open symbols: kinetic model 2. Solid symbols: kinetic model 3.

kinetic regime),  $C_B/C_{B_0}$  changes from 0.28 to 0.78 when kinetic model 2 and 3, respectively, are applied. However, when  $k_D = 10 \text{ M}^{-1}\text{s}^{-1}$  (slow kinetic regime) differences only increase from 0.95 to 0.97 and there are no differences when  $k_D = 1 \text{ M}^{-1}\text{s}^{-1}$  (not shown). This means that for values of  $k_D$  leading to slow kinetic

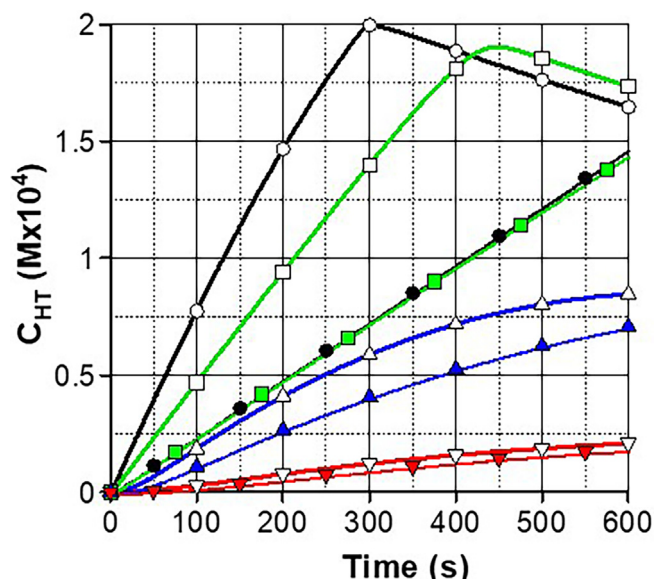


**Fig. 13.** Evolution of hydrogen peroxide initial concentration in the ozonation of a generic compound (B). Conditions:  $C_{O_3\text{gin}} = 2 \times 10^{-4}$  M,  $\text{pH} = 7$ ,  $\beta = 0.98$ ,  $k_{l,a} = 2 \times 10^{-4} \text{ s}^{-1}$ ,  $k_l = 5 \times 10^{-5} \text{ m}^2 \text{ s}^{-1}$ ,  $V = 1.0 \text{ L}$ ,  $Q_g = 20 \text{ L h}^{-1}$ ,  $C_{B_0} = 2 \times 10^{-4}$  M. Direct rate constant ozone-B reaction:  $\bullet$  (black line),  $10^6 \text{ M}^{-1}\text{s}^{-1}$ ;  $\square$  (green line),  $10^4 \text{ M}^{-1}\text{s}^{-1}$ ;  $\triangle$  (blue line),  $10^2 \text{ M}^{-1}\text{s}^{-1}$ ;  $\nabla$  (red line),  $10 \text{ M}^{-1}\text{s}^{-1}$ . Open symbols: kinetic model 2. Solid symbols: kinetic model 3.

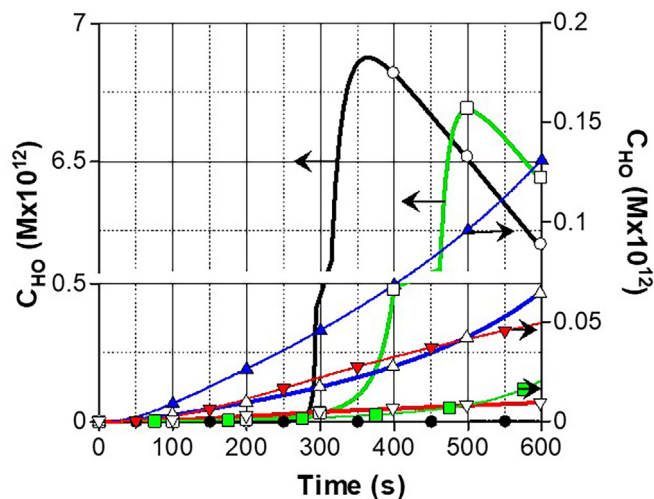


**Fig. 14.** Evolution with time of calculated bulk hydroxyl radical concentration in the ozonation of a generic compound (B). Effect of  $k_D$ . Conditions:  $C_{O_3\text{gin}} = 2 \times 10^{-4}$  M,  $\text{pH} = 7$ ,  $\beta = 0.98$ ,  $k_{l,a} = 2 \times 10^{-4} \text{ s}^{-1}$ ,  $k_l = 5 \times 10^{-5} \text{ m}^2 \text{ s}^{-1}$ ,  $V = 1.0 \text{ L}$ ,  $Q_g = 20 \text{ L h}^{-1}$ ,  $C_{B_0} = 2 \times 10^{-4}$  M. Direct rate constant of ozone-B reaction:  $\bullet$  (black line),  $10^6 \text{ M}^{-1}\text{s}^{-1}$ ;  $\square$  (green line),  $10^4 \text{ M}^{-1}\text{s}^{-1}$ ;  $\triangle$  (blue line),  $10^2 \text{ M}^{-1}\text{s}^{-1}$ ;  $\nabla$  (red line),  $10 \text{ M}^{-1}\text{s}^{-1}$ . Open symbols: kinetic model 2. Solid symbols: kinetic model 3.

regimes, the influence of film reactions is practically negligible which confirms the results calculated from the application of the film theory (see Fig. 2), though film theory results refer to starting conditions. Another important question is to assess the effect of free radical reactions in the film layer. For so doing, kinetic model 4 that only considers the direct reaction in the film and both direct and free radical reactions in the water bulk, was tested. From Fig. 11, it is observed that only after some reaction period (about 200 s) the absence of free radical reactions in the film leads to a slight decrease in the removal rate of B in the fast kinetic regime ( $k_D = 10^6 \text{ M}^{-1}\text{s}^{-1}$ ). However, in the case of slow regimes ( $k_D = 10$ -

$\text{M}^{-1}\text{s}^{-1}$ ) these differences are lower and negligible in a slow reaction ( $k_D = 10 \text{ M}^{-1}\text{s}^{-1}$ ). The negligible or null differences at the start of reactions also confirms the results from the film theory as indicated in section 2.1. Also from Fig. 11, the absence of differences between concentrations calculated from kinetic model 3 for  $k_D = 10^6$  and  $10^4 \text{ M}^{-1}\text{s}^{-1}$  is noticed. These apparent contradictory results are due to the shortage of ozone supplied ( $C_{\text{O}_3\text{ge}} = 2 \times 10^{-4} \text{ M}$ ). Differences are observed if  $C_{\text{O}_3\text{ge}}$  is increased (results not shown).

From Fig. 12, the effect of  $k_D$  on the dissolved ozone concentration with time is shown. It can be seen that the concentration of dissolved ozone is always lower when film reactions are not considered which is in accordance to Fig. 11 showing B concentration profiles. When film reactions are not considered, the amount of B present in water is more significant and, as a consequence, ozone consumption increases so that its bulk concentration is lower than in the case where film reactions are taken into account. There is an exception when fast reactions develop ( $k_D = 10^4 - 10^6 \text{ M}^{-1}\text{s}^{-1}$ ). In these cases, there is an initial period of time (300 s) needed to complete the removal of B (Fig. 11). In this period dissolved ozone concentration is negligible, regardless of the kinetic model applied. However, after this reaction time, the pattern observed is similar to the one obtained for lower  $k_D$  values. This is in accordance with results shown in Fig. 2 from film theory and fast reaction. Fig. 2 reveals that negligible dissolved ozone reaches the film-bulk water interface, while the opposite situation is observed for slow reaction ( $k_D \leq 100 \text{ M}^{-1}\text{s}^{-1}$ ).

Regarding the time bulk concentration profiles of ozone in the gas leaving the reactor (see Figure S4), it is seen that, at a given time, the presence of film reactions, compared to their absence, leads to lower concentrations of ozone in the outlet gas. This is a consequence of the high dissolved and consumed ozone due to the film reactions. Accordingly, not considering film reactions in the kinetic model would lead to predict a higher ozone loss. This is specially important when fast-moderate ozone reactions develop. For slow reactions lower differences are observed between both kinetic models.

Fig. 13 presents the changes of bulk concentration of hydrogen peroxide with time at different  $k_D$ . It is observed that kinetic model 2 leads to higher concentrations of hydrogen peroxide than kinetic model 3 because of the contributions of film reactions (specially the direct reaction (1)). Also, for fast reactions, concentration reaches a maximum value at a time where total removal of B is achieved (300 s when  $k_D = 10^6 \text{ M}^{-1}\text{s}^{-1}$ ). The difference, however, is negligible when the slow kinetic regime occurs ( $k_D = 10 \text{ M}^{-1}\text{s}^{-1}$ ) because negligible reactions proceed in the film layer.

Fig. 14 displays the changes with time of hydroxyl radical concentration (responsible oxidant of indirect reaction (8)) at different  $k_D$  values. It is observed that while B is in solution kinetic model 2 predicts lower hydroxyl radical concentrations than kinetic model 3. This is likely due to the higher hydroxyl radical consumption when film reactions are considered. However, in the absence of B, which happens in fast-moderate reactions at 300–400 s, hydroxyl radicals increase when film reactions are considered, and the concentration becomes higher than that predicted from kinetic model 3. This is due to the initiation reaction (3) through which, in the absence of B, most ozone reacts with hydrogen peroxide to yield free radicals. Differences in concentrations are very low for slow kinetic regimes. Similarly to hydrogen peroxide evolution, there is also a maximum concentration of hydroxyl radicals reached once B has disappeared with  $k_D$  values corresponding to fast-moderate kinetic regimes. Differences, however, do not affect the removal rates of B since the direct reaction (1) is the only responsible step through which B disappears. Film reactions, instead, do affect the changes of hydrogen peroxide, ozone, and hydroxyl radical concentrations.

### Influence of $C_{\text{B}_0}$

Concentration of compound B affects both the Hatta number and the instantaneous reaction factor,  $E_i$ . Accordingly,  $C_{\text{B}_0}$  influence was studied and shown in Fig. 11 and S5 to S8 for data from kinetic model 2. As seen from Fig. 11, at a given time, conversion of B is higher when  $C_{\text{B}_0}$  is lower, but the corresponding removal rate obviously decreases with the decrease of  $C_{\text{B}_0}$ . Also, in Fig. 11, as observed for curves corresponding to  $k_D = 10^6 \text{ M}^{-1}\text{s}^{-1}$ , both conversion and removal rate of B from kinetic model 2 are much higher than those from kinetic model 3 which confirm the importance of film reactions.

Regarding ozone concentrations with time, as observed from Figures S5 and S6, the increase of B initial concentration leads, as expected, to lower concentrations of ozone (in gas and in water) as a consequence of reaction (1). During the first minutes of ozonation, influence of reaction (1) is particularly important at the highest initial concentrations of B (see curves for  $C_{\text{B}_0} = 2 \times 10^{-4} \text{ M}$  in Fig. 12 and for  $C_{\text{B}_0} = 8 \times 10^{-5} \text{ M}$  in Figure S5) where no dissolved ozone is observed. At these conditions, the ozone-B direct reaction (1) is a fast ozone reaction and negligible amount of ozone reaches the water bulk (see also Fig. 2).

In Figures S7 and S8 the effect of  $C_{\text{B}_0}$  on time bulk concentrations of hydrogen peroxide and hydroxyl radicals is presented. From Figure S7 it is seen that the concentration of hydrogen peroxide presents a positive effect of  $C_{\text{B}_0}$  on its formation, consequence of the importance of reaction (1). In the case of hydroxyl radicals, as shown in Figure S8, during the first seconds of reaction, a negative effect of  $C_{\text{B}_0}$  is observed consequence of reaction (8). Once this first reaction period has elapsed and the process reaches a stationary state,  $C_{\text{B}_0}$  positively affects the formation of hydroxyl radicals since reaction (3) predominates over consumption reactions of hydroxyl radical (reactions (8) to (12)). At these reaction times, there is less B present in water and ozone is mainly consumed through reaction (3).

As a result of the information obtained, definitively, film reactions must be included in any kinetic model of ozonation. However, the effect of free radical reactions in the proximity of gas-water interface has negligible effect on the removal of B. In any case, film reactions do have significant influence on the formation of hydrogen peroxide and hydroxyl radicals. In any case, the decrease of  $C_{\text{B}_0}$  leads to a faster disappearance of this compound but with lower removal rates regardless of the application of kinetic model 2 or 3. Differences are significant and negligible when fast-moderate reactions and slow reactions develop, respectively.

### Influence of hydrogen peroxide addition and pH

The simultaneous presence of ozone and hydrogen peroxide, especially when the latter is added, constitutes the first ozone involving AOP reported [32]. When hydrogen peroxide is added, the rate of initiation reaction (3) is increased, especially, at high pH. In Figure S9, the effect of hydrogen peroxide addition on the time concentration profiles from kinetic models 2 and 3 are shown. For the mechanism considered, addition of hydrogen peroxide up to a concentration of 0.01 M does not alter the removal rate of B (see top left of Figure S9). Kinetic model 3 also predicts similar but lower concentrations of hydrogen peroxide with time for different concentrations of added hydrogen peroxide. Figure S9 (bottom left) reveals that increasing the added concentration of hydrogen peroxide leads to a positive net formation of this compound. Once a maximum value is reached (when B is totally removed), net formation rate of hydrogen peroxide is negative with values that increase with the increasing initial concentration added. This is a consequence of the high reaction rate with both

ozone and mainly hydroxyl radicals. Contrarily to B and H<sub>2</sub>O<sub>2</sub> profiles, concentrations of ozone (in gas and water) do diminish with the increasing addition of hydrogen peroxide, likely due to reaction (3). However, in absence of film reactions the time concentration profile of ozone (in gas and in water) do not depend on added hydrogen peroxide. In this case, as expected, ozone concentration in the gas is much higher from kinetic model 3.

Regarding bottom left of Figure S9, from kinetic model 3, it is seen that while B is in water, concentration of hydroxyl radicals is lower than 10<sup>-13</sup> M. Hydroxyl radicals are mainly consumed by hydrogen peroxide. In the absence of B, ozone reacts with hydrogen peroxide to yield decreasing concentrations of hydroxyl radicals with the increase of added hydrogen peroxide. This is due to the scavenging character of hydrogen peroxide through reactions (10) and (11). Accordingly, the addition of hydrogen peroxide should be limited to an optimum value. Results from kinetic model 3 leads to similar conclusions as presented above though hydroxyl radical concentrations are about three order of magnitude lower than from kinetic model 2. Therefore, Inclusion of film reactions (especially the direct reaction) is compulsory to have correct predictions on time concentration profiles for fast-moderate ozone-B reactions.

Finally, the effect of another important variable of ozone processes, pH, was also studied, the results being shown in Figure S10 for the case of a fast ozone direct reaction ( $k_D = 10^6 \text{ M}^{-1}\text{s}^{-1}$ ). Application of kinetic model 2 predicts no effect of pH on the concentration of B (only at pH 11 differences start to be observed from 200 s) while use of kinetic model 3, at a given time, leads to lower concentrations of B with negligible pH effect (see top left Figure S10). In the absence of film reactions, ozone gas concentration does not change with pH, however, if film reactions are considered, while B is in water (up to 300 s) concentration of ozone in the gas is lower than that observed from kinetic model 3 and does not depend on pH either. For pH 11, ozone gas concentration is lower, due to the higher importance of initiation reaction (3) (top middle Figure S10). For ozone dissolved in water, pH between 9 and 11 also seems to be the frontier to observe an effect of pH. In the presence of film reactions, once B has been removed, ozone concentration increases with the decreasing pH due to reaction (3). Regarding hydrogen peroxide (see bottom left in Figure S10), in the presence of film reactions, and B in water, no pH effect is observed. Once B has disappeared, there is an increasing rate of hydrogen peroxide removal with increasing pH as a consequence of reactions (3), (10) and (11). Regardless of reaction time, at pH 11, hydrogen peroxide is always lower. In the absence of film reactions, it is seen a continuous increment of hydrogen peroxide concentration with time. This concentration does not depend on pH except at pH 11 that leads to even lower concentrations. These concentrations are in any case lower than those predicted from kinetic model 2. Finally, from bottom right of Figure S10, the effect of pH on the formation of hydroxyl radicals is presented. In any case, the presence of film reactions, kinetic model 2, leads to concentrations between two and three order of magnitude higher than in their absence.

#### Influence of $k_T$

A priori, another important variable is the scavenging effect of the water to capture hydroxyl radicals and diminishing their competitive action on B through reaction (8). This effect can be checked changing the value of  $k_T = k_5C_5$ . A typical natural scavenger is the bicarbonate/carbonate system. Assuming a mean concentration of 10<sup>-3</sup> M and given the values of the rate constants of the reaction between hydroxyl radical and both forms of carbonates,  $k_T$  can be taken as about 10<sup>4</sup> s<sup>-1</sup> (Beltrán, 2004). With this value kinetic models 2 and 3 were checked (see some results are shown in Figure S11). As it can be seen, regardless of the ozone-B reaction is

fast or slow there are no differences in concentrations by varying  $k_T$ , except in two cases once B has been removed (300 s). These cases refer to concentrations of dissolved ozone (Figure S11, top right) and hydroxyl radical (Figure S11, bottom right) and when kinetic model is applied. In the first case, there is a slight increase of ozone concentration, which is undoubtedly due to the stabilization of ozone because the scavenger hydroxyl radical trapping through reaction (12). This makes reaction (9) be partially inhibited. In the second case, concentration of hydroxyl radicals significantly decreases in the presence of scavengers also due to termination reaction (12). Concentrations of scavengers can rise as much as another order of magnitude but neither at these conditions their presence will have an effect on fast-moderate reactions and regardless film reactions are considered. Only in the case, of very slow reactions ( $k_D < 0.1 \text{ M}^{-1}\text{s}^{-1}$ ) some differences could be observed to slow the removal of B.

#### Conclusions

Main conclusions that can be extracted from this work are:

Dimensionless parameters, such as Hatta number and instantaneous reaction factor are fundamental to predict according to film theory if film ozone reactions will have a significant effect of the ozonation rate of a generic compound B.

Kinetic models of ozone reactions in water have to include direct and hydroxyl radical reactions in the proximity of gas-water interface or film layer. Absence of these reactions in the kinetic model leads to lower removal rates of target compounds, especially for fast-moderate ozone reactions.

The effects of film direct reactions are more important with increasing values of direct rate constants and decreasing values of the mass transfer coefficient. In other words when kinetic regimes of ozone reactions are fast or moderate. These effects are negligible in the case of slow reactions.

The absence of film free radical reactions while keeping film direct reactions (kinetic model 4) at advanced reaction times, leads to slightly slower removal of compound B, mainly due to the absence of ozone consumption in competitive reactions with hydrogen peroxide and free radicals.

Concentrations of free radicals from film reactions are in any case low to have a participating role in the removal rate of target compound specially in fast-moderate kinetic regimes. Only at advanced reaction times, some effect is observed.

Effects of other variables, such as B concentration, pH and hydrogen peroxide leads to similar conclusions regarding removal rates of target compound (B). Also, concentrations of hydrogen peroxide and hydroxyl radicals are higher when film reactions are considered but have little or no effect on B removal for fast-moderate reactions.

The conclusions deduced in this work will be applied in the next future to study the kinetic modelling of the water ozonation of actual organic contaminants.

#### Declaration of Competing Interest

The authors declare that they have no known competing financial interests or personal relationships that could have appeared to influence the work reported in this paper.

#### Acknowledgements

Authors thank the Agencia Estatal de Investigación of Spain (PID2019-104429BI00/MCIN/AEI/10.13039/501100011033) for the economic support.

## Funding

This work was economically supported by the Agencia Estatal de Investigación of Spain (PID2019-104429RBI00/MCIN/AEI/10.13039/501100011033).

## Appendix A. Supplementary data

Supplementary data to this article can be found online at <https://doi.org/10.1016/j.jiec.2023.07.001>.

## References

- [1] M. Zhu, N. Gao, W. Chu, S. Zhou, Z. Zhang, Y. Xu, Q. Dai, *Ecotoxicol. Environ. Saf.* 120 (2015) 256–262, <https://doi.org/10.1016/j.ecoenv.2015.05.048>.
- [2] G. Hua, D.A. Reckhow, *Water Res.* 47 (13) (2013) 4322–4330, <https://doi.org/10.1016/j.watres.2013.04.057>.
- [3] C.A. Morales-Paredes, J.M. Rodríguez-Díaz, N. Boluda-Botella, *Sci. Total Environ.* 814 (2022), <https://doi.org/10.1016/j.scitotenv.2021.152691>.
- [4] X. Liu, Z. Yang, W. Zhu, Y. Yang, H. Li, *J. Environ. Manage.* 319 (2022), <https://doi.org/10.1016/j.jenvman.2022.115662>.
- [5] M.I. Pariente, Y. Segura, S. Álvarez-Torrellas, J.A. Casas, Z.M. de Pedro, E. Diaz, J. García, M.J. López-Muñoz, J. Marugán, A.F. Mohedano, R. Molina, M. Munoz, C. Pablos, J.A. Perdigón-Melón, A.L. Petre, J.J. Rodríguez, M. Tobajas, F. Martínez, *J. Environ. Manage.* 320 (2022), <https://doi.org/10.1016/j.jenvman.2022.115769>.
- [6] O. Porcar-Santos, A. Cruz-Alcalde, B. Bayarri, C. Sans, *Sci. Total Environ.* 846 (2022), <https://doi.org/10.1016/j.scitotenv.2022.157173>.
- [7] Y. Sun, M. Li, M.H. Hadizadeh, F. Xu, *J. Environ. Chem. Eng.* 11 (1) (2023), <https://doi.org/10.1016/j.jece.2022.109167>.
- [8] E.C. Wert, F.L. Rosario-Ortiz, D.D. Drury, S.A. Snyder, *Water Res.* 41 (7) (2007) 1481–1490, <https://doi.org/10.1016/j.watres.2007.01.020>.
- [9] J.F. Maria, L. Bonnie, V.G. A. de, S. Daniel, G. Wolfgang, *J. Environ. Eng.* 142 (3) (2016) 4015087, [https://doi.org/10.1061/\(ASCE\)EE.1943-7870.0001022](https://doi.org/10.1061/(ASCE)EE.1943-7870.0001022).
- [10] Y.A. Oktem, B. Yuzer, M.I. Aydin, H.E. Okten, S. Meric, H. Selcuk, *J. Environ. Manage.* 247 (2019) 749–755, <https://doi.org/10.1016/j.jenvman.2019.06.114>.
- [11] P. Loganathan, J. Kandasamy, S. Jamil, H. Ratnaweera, S. Vigneswaran, *Chemosphere* 296 (2022), <https://doi.org/10.1016/j.chemosphere.2022.133961>.
- [12] S. Psaltou, M. Mitrakas, A. Zouboulis, *Separations* 9 (7) (2022) 173, <https://doi.org/10.3390/separations9120413>.
- [13] Z. Li, J. Wang, J. Chang, B. Fu, H. Wang, *Sci. Total Environ.* 857 (2023), <https://doi.org/10.1016/j.scitotenv.2022.159172>.
- [14] A. Saravanan, V.C. Deivayanai, P.S. Kumar, G. Rangasamy, R.V. Hemavathy, T. Harshana, N. Gayathri, K. Alagumalai, *Chemosphere* 308 (2022), <https://doi.org/10.1016/j.chemosphere.2022.136524>.
- [15] Y.S. Zimin, G.G. Kutlugildina, G.M. Sharipova, *React. Kinet. Mech. Catal.* 135 (6) (2022) 2929–2944, <https://doi.org/10.1007/s11144-022-02302-x>.
- [16] Y. Ma, J. Wang, H. Wang, C. Wang, C. He, X. Zhang, *Process Saf. Environ. Prot.* 167 (2022) 67–76, <https://doi.org/10.1016/j.psep.2022.09.006>.
- [17] J.-C. Charpentier, in: T. B. Drew, G. R. Cokelet, J. W. Hoopes, T. B. T.-A. in C. E. Vermeulen (Eds.), Vol. 11, Academic Press, 1981, pp. 1–133.
- [18] V. Štěpánek, Z. Palatý, H. Bendová, *Chem. Eng. Sci.* 191 (2018) 410–419, <https://doi.org/10.1016/j.ces.2018.07.003>.
- [19] D.A. Glasscock, G.T. Rochelle, *AIChE J.* 35 (8) (1989) 1271–1281, <https://doi.org/10.1002/aic.690350806>.
- [20] H. Benbelkacem, H. Debellefontaine, *Chem. Eng. Process. Process Intensif.* 42 (10) (2003) 723–732, [https://doi.org/10.1016/S0255-2701\(02\)00074-0](https://doi.org/10.1016/S0255-2701(02)00074-0).
- [21] A.M. Chávez, F.J. Beltrán, J. López, F. Javier Rivas, P.M. Álvarez, *Chem. Eng. J.* 458 (2023), <https://doi.org/10.1016/j.cej.2023.141408>.
- [22] F.J. Beltran, *Ozone reaction kinetics for water and wastewater systems*, CRC Press, 2003.
- [23] Z. Qiang, C. Adams, R. Surampalli, *Ozone Sci. Eng.* 26 (6) (2004) 525–537, <https://doi.org/10.1080/01919510490885334>.
- [24] M.C. Dodd, M.O. Buffle, U. Von Gunten, *Environ. Sci. Technol.* 40 (6) (2006) 1969–1977, <https://doi.org/10.1021/es051369x>.
- [25] D.W. van Krevelen, P.J. Hoftijzer, *Recl. Des Trav. Chim. Des Pays-Bas* 67 (7) (1948) 563–586, <https://doi.org/10.1002/recl.19480670708>.
- [26] J.L. Sotelo, F.J. Beltrán, F.J. Benitez, J. Beltrán-Heredia, *Water Res.* 23 (10) (1989) 1239–1246, [https://doi.org/10.1016/0043-1354\(89\)90186-3](https://doi.org/10.1016/0043-1354(89)90186-3).
- [27] P.N. Johnson, R.A. Davis, *J. Chem. Eng. Data* 41 (6) (1996) 1485–1487, <https://doi.org/10.1021/je9602125>.
- [28] P.M. Doran, in: P. M. B. T.-B. E. P. (Second E. Doran (Ed.), Academic Press, London, 2013, pp. 379–444.
- [29] M. Sievers, in: P. B. T.-T. on W. S. Wilderer (Ed.), Elsevier, Oxford, 2011, pp. 377–408.
- [30] H. El Abd, A. Hafez, E. El Zanati, G. El Diwani, *Environ. Int.* 11 (6) (1985) 493–498, [https://doi.org/10.1016/0160-4120\(85\)90183-7](https://doi.org/10.1016/0160-4120(85)90183-7).
- [31] R. Higbie, *Trans. AIChE* 31 (1935) 365–369.
- [32] W.H. Glaze, J.-W. Kang, D.H. Chapin, *Ozone Sci. Eng.* 9 (4) (1987) 335–352, <https://doi.org/10.1080/01919518708552148>.